



Published in final edited form as:

Respirology. 2011 February ; 16(2): 340–349. doi:10.1111/j.1440-1843.2010.01910.x.

Ambient particulate matter affects occludin distribution and increases alveolar transepithelial electrical conductance

Juan C Caraballo^{*}, Cecilia Yshii^{*}, Whitney Westphal^{*}, Thomas Moninger[†], and Alejandro P Comellas^{*}

^{*}University of Iowa, Internal Medicine Department, Iowa City, Iowa

[†]University of Iowa, Central Microscopy Research Facility, Iowa City, Iowa

Summary at a glance

This work studies the effects of particulate matter and diesel exhaust particles on alveolar barrier integrity *in vitro*. Our results show that these particles alter tight junction integrity, specifically the Occludin and ZO-1 association. These effects are prevented by blocking of mitochondrial ROS production, suggesting a central role of this organelle in the effects observed.

Background and objective—Inhaled particulate matter (PM) causes lung inflammation and epithelial dysfunction. However, the direct effect of PM on alveolar epithelial barrier integrity is not well understood. Our aim is to determine whether PM exposure affects the alveolar epithelial cells (AEC) transepithelial electrical conductance (*Gt*) and tight junction (TJ) proteins.

Methods—Human AEC (A549) and primary rat AEC were exposed to PM of <10 μm in size (PM₁₀) and diesel exhaust particles (DEP), using titanium dioxide (TiO₂) as a control for particle size effects. *Gt* and permeability to fluorescein isothiocyanate-dextran (FITC-dextran) were measured to assess barrier integrity. TJ integrity was evaluated by analyzing penetration of Lanthanum nitrate (La³⁺) under transmission electron microscopy. Surface proteins were labeled with biotin and analyzed by Western blot (WB). Immunofluorescence was performed to assess co-localization of TJ proteins including occludin and zonula occludens-1 (ZO-1). PM induced dissociation of occludin-ZO-1 was evaluated by co-immunoprecipitation.

Results—PM₁₀ and DEP increased *Gt* and disrupted TJ after 3h of treatment. PM₁₀ and DEP induced occludin internalization from the plasma membrane into endosomal compartments and dissociation of occludin from ZO-1. Overexpression of antioxidant enzymes Manganese Superoxide Dismutase (MnSOD) and Catalase, prevented PM-induced *Gt* increase, occludin reduction from the plasma membrane and its dissociation from ZO-1.

Conclusions—PM induces alveolar epithelial dysfunction in part via occludin reduction at the plasma membrane and ZO-1 dissociation in AEC. Furthermore, these effects are prevented by overexpression of two different antioxidant enzymes.

Keywords

Occludin; particulate matter; pneumocytes; reactive oxygen species; zonula occludens 1-protein

Introduction

Strong epidemiological data links ambient particulate matter (PM) to morbidity and mortality due to cardiopulmonary diseases¹⁻³. Acute exposure to PM is associated with an increase in daily mortality, asthma and COPD exacerbations⁴⁻⁷. Furthermore, exposure to extraordinary high levels of PM, such as indoor air pollution from the use of biomass fuel^{8,9} and during historic episodes of severe airborne pollution in Pennsylvania (1948) and London (1952)¹⁰, affects significantly lung function and health. More recently, rescue workers at the world trade center showed substantial loss in pulmonary function during the first year after the event (2001)¹¹, and Aldrich et al reported that this loss of pulmonary function was not recovered after 7 years from the original event¹².

The alveolar epithelium serves as a physical barrier and part of innate immunity against inhaled particles and microorganisms¹³. Accordingly, alveolar epithelial dysfunction plays an important role in the development of lung injury. However, there is a paucity of data regarding the direct effects of PM on the integrity of the alveolar epithelial barrier. A functional alveolar epithelial barrier requires the formation of intercellular interactions via cell adhesion proteins¹⁴. These include E-cadherin and tight junctions (TJ). TJ are the most apical junction and delineate the apical and basolateral surface of epithelial cells. It has been reported that air pollutants alter Occludin distribution in airway epithelial cells¹⁵.

We hypothesize that PM induces an increase in ROS generation, leading to a reorganization of TJ proteins and development of a dysfunctional alveolar epithelial barrier. In order to test this, we set out to determine the effect of PM on primary rat and human AEC, measuring transepithelial electrical conductance (Gt), an indicator of epithelial barrier integrity, and cell adhesion proteins abundance at the plasma membrane.

Methods

A more detailed description is provided in the supplementary data section.

Particles and reagents

All reagents were purchased from Sigma-Aldrich (St Louis, MO) unless indicated otherwise. Particulate matter <10 μ m diameter (PM₁₀) and Diesel exhaust particles (DEP) were purchased from National Institute of Standards and Technology (Gaithersburg, MD). Particles were suspended in DMEM at room temperature and sonicated for 10 sec to avoid aggregation.

Cells

Primary rat alveolar type II epithelial cells were isolated from male Sprague Dawley rats as previously described¹⁶. Day of isolation is designated as Day 0, cells were used day 3 and 4. Human alveolar epithelial cells (A549) were obtained from ATCC. ρ 0 cells were generated by incubating A549 cells in medium containing ethidium bromide (50ng/ml), sodium pyruvate (1mM), and uridine (50 μ g/ml) for 4–6 weeks¹⁷. Use of animal was approved by the Animal Care and Use Committee of the University of Iowa.

Transepithelial Electrical Conductance (Gt)

Transepithelial electrical resistance (Rt) was measured with Millicell Electrical Resistance System (ERS) (Millipore Corporation, Bedford, MA) and Gt was calculated as the reciprocal of Rt .

Lanthanum nitrate

After treatment, cells were fixed and then incubated with a 1:1 solution of 0.2M Lanthanum Nitrate and 0.2M Sym-Collidine with 2% Osmium tetroxide on the apical side. 0.2M Sym-Collidine was maintained without Lanthanum nitrate in the basolateral side of the cells. The cells were then dehydrated and embedded in resin. Sections were observed under transmission electron microscope (TEM).

Adhesion of cells to E-Cadherin-Fc

E-cadherin dependent adhesion of cells to E-cadherin coated plates was assed as described by Zabner et al¹⁸. Cells were labeled with Calcein-AM (5ng/ml) and incubated for 30min at 37°C. Cells were then harvested and plated on E-cadherin coated plates and allowed to bind for 45min at 37°C. Cells were treated with PM₁₀ for 3h and then wells were washed to remove detached cells from the plate. Fluorescence was measured to assess the remaining amount of cells attached to the plate.

Cell surface biotinylation

After treatments, cell surface proteins were labeled using 1mg/ml EZ-link NHS-SS-Biotin (Pierce Chemical, Rockford, IL). Thereafter, cells were harvested and 100ug of cell lysate proteins were incubated overnight at 4°C with streptavidin beads with end-over-end rotation. Biotinylated proteins were eluted from the beads and analyzed with SDS-PAGE.

Adenovirus infection

Cells were infected with 20pfu/cell of adenovirus, empty or containing the plasmid of interest (e.g. MnSOD (Ad5CMVMnSOD) and Catalase (Ad5CMVCat) (gifts from Dr. J. Engelhardt, through University of Iowa, Viral Core))^{19,20}. Inducible Bcl-xL adenovirus (gift from Dr. Budinger GR, Northwestern University).

Immunofluorescence

After treatment, cells were fixed and immunofluorescence labeling was performed by exposing cells to primary antibodies, using monoclonal anti-occludin and polyclonal anti-ZO-1 (Invitrogen, Carlsbad, CA). Cells were then exposed to Cy3-coupled goat anti-rabbit and FITC-coupled goat anti-mouse antibodies (Invitrogen). Cells were visualized under confocal fluorescence microscope.

Statistics

Comparison between experimental groups was made with one way ANOVA test. The unpaired Student t-test was used to test for significance. Statistical significance was set as p-value <0.05. Data is shown as mean ± SE.

Results

PM induces alveolar epithelial dysfunction independently of cell death/injury

We determined whether PM disrupts the alveolar epithelial barrier by examining the effect of PM₁₀ on 4kDa FITC-Dextran permeability and *Gt* in primary rat AEC. *Gt* is an indicator of ion flux through the epithelium, hence of barrier integrity. Unlike human AEC, primary rat AEC are capable of forming TJ when cultured, making it possible to assess *Gt*. Primary rat AEC were plated on inserts and permeability to FITC-Dextran was measured by determining the basolateral/apical ratio (B/A) of fluorescence at different time points. As shown in Figure 1A, PM₁₀ increased the permeability to FITC-dextran after 24h of exposure. In addition, exposure to PM₁₀ (50µg/cm²) increased *Gt* in a time-dependent

manner, becoming statistically significant after 2h of treatment (Fig. 1B). Our dose of suspension particles is comparable to that used by previous authors that have studied other effects of PM on lung epithelial cells²¹⁻²³, and could be equivalent to lower doses when exposed in air-liquid interface²⁴.

Death of conforming cells of a monolayer can lead to disruption of the epithelial barrier. PM induces p53 expression and apoptosis of AEC at 24 hours²⁵. We examined the role of cell death in PM-induced changes in permeability and *Gt*. Cell death, measured by LDH release and propidium iodide fluorescence, was not significantly different after 3h of PM₁₀ and DEP treatment when compared to TiO₂ and control (data not shown), suggesting that changes in *Gt* observed at 3h are not a consequence of cell death. Furthermore, we infected AEC with adenovirus with B-cell lymphoma-extra large (Bcl-xL) gene, in order to prevent apoptosis²⁶ (Supplementary data Fig. 1S). As shown in Figure 1C, overexpression of Bcl-xL prevented the PM-induced increase of FITC-dextran permeability after 24h of treatment but failed to prevent PM-induced increase of *Gt* at 3h (Fig. 1D).

To further study paracellular permeability, La³⁺ movement through the TJ was evaluated in primary rat AEC using transmission electron microscopy (TEM) as described by Flynn et al²⁷. La³⁺ is an electron dense element with a radius of 0.4nm and TJ are impermeable to it under normal conditions. Since TiO₂ is an inert particle, it was used as a control in these experiments to discern whether particles themselves have an effect on paracellular permeability in primary rat AEC. DEP form part of PM₁₀ and are able to reach the alveolar space due to their small size. Consequently, we decided to test the effect of DEP on the alveolar epithelial barrier as well. As shown in Figure 1E, exposure to PM₁₀ and DEP for 3h caused La³⁺ to pass through the intercellular space, while AEC treated with TiO₂ remained impermeable to the tracer.

PM decreases membrane occludin, but it does not affect other tight or adherens junction proteins

The effect of PM₁₀ on several cell adhesion proteins was examined. After 3h of treatment, surface proteins were analyzed by western blot (WB) and immunofluorescence (IF) staining. PM₁₀ did not affect the abundance at the plasma membrane of E-Cadherin, or Claudin 5, 3 & 18 (see supplementary Fig. 2S).

Although there was no change observed in the amount of surface E-cadherin in AEC, we decided to assess the effect of PM on physical adhesion of E-cadherin, since the integrity of the adherens junctions can influence the integrity of the TJ^{28, 29}. Adherens junction adhesion was determined as previously described by Zabner et al¹⁸ (see methods). As shown in Figure 2A, PM₁₀ did not affect the adhesion of cells to E-cadherin coated plates, while treatment with ethylenediaminetetraacetic acid (EDTA), a calcium chelator, or pretreatment of plates with an E-cadherin blocking antibody (RR1), significantly reduced the proportion of cells that remained attached to the plate. Accordingly, PM neither affects the quantity of E-Cadherin on the membrane nor the capacity of this protein to form homologous associations.

As shown in Figure 2B, exposure to PM₁₀ significantly decreased occludin abundance at the plasma membrane after two hours of treatment. Exposure to PM₁₀ and DEP for 3h reduced occludin abundance at the plasma membrane, in primary rat AEC as well as in human AEC (A549) (Fig. 2C). Despite this the latter cannot form adequate TJ in culture. However, total abundance of occludin is not altered by any of the treatments, as shown in Figure 2D.

Occludin is incorporated into endosomal compartments after exposure to PM

Endosomal compartment was separated by sucrose gradient³⁰. This fraction was then analyzed by WB in order to determine whether reduced surface occludin correlates with an increase in the endosome. Chloroquine pretreatment was required in order to inhibit lysosomal degradation of occludin and allow its accumulation in endosomal compartments. As shown in Figure 3A, occludin increased in the endosomal compartment of pretreated human AEC exposed to PM₁₀ for 3h. Chloroquine treatment alone did not affect the PM-induced *Gt* increase (Fig. 3B), nor PM-induced decrease in plasma membrane occludin abundance in AEC (Supplementary Fig. 3S).

PM-induced *Gt* increase and reduction of occludin abundance at the plasma membrane is prevented by overexpression of antioxidant enzymes

Mitochondrial ROS production plays an important role in the PM-induced effects on AEC, such as cell death, nuclear factor kappa-B (NF- κ B) activation, and inflammation^{22,31}. We investigated the role of the mitochondria on the effects of PM₁₀ on occludin abundance at the plasma membrane in A549- ρ 0 (ρ 0) cells, which lack the necessary enzymatic machinery to generate mitochondrial ROS^{29,32}. As shown in Figure 4A, PM₁₀ exposure for 9 hours substantially decreased the occludin abundance at the plasma membrane, while ρ 0 cells did not show any reduction. Furthermore, we infected cells with adenovirus containing plasmids with genes for MnSOD and Catalase, antioxidant enzymes localized respectively in the mitochondria and cytosol (Supplementary Fig. 4S). Overexpression of these enzymes prevented PM-induced *Gt* increase (Figure 4B), and reduction of occludin abundance at the plasma membrane in AEC (Figure 5A and 5B). These results suggest a role of mitochondrial ROS in PM-induced *Gt* increase and occludin reduction at the plasma membrane in AEC.

PM induced occludin and ZO-1 dissociation is prevented by overexpression of MnSOD and Catalase

Occludin is bound to cytoskeleton primarily by its association with ZO-1, representing an important component of TJ architecture. Primary rat AEC were grown on inserts and treated with TiO₂, PM₁₀ and DEP for 3h; confocal microscopy was then performed. As shown in Figure 6, treatments with PM₁₀ and DEP but not TiO₂ reduced the colocalization of occludin and ZO-1. The effect of PM on the association between ZO-1 and occludin was also determined by co-immunoprecipitation. As shown in Figure 7A, PM₁₀ and DEP decrease the association between these two proteins, compared with control and TiO₂ treatments. In addition, Overexpression of MnSOD or Catalase prevented this effect (Fig. 7B).

Discussion

Our results show that PM induces an increase in *Gt*, a reduction of occludin abundance at the plasma membrane and its dissociation from ZO-1, without affecting other TJ proteins such as claudins or the adherens junction, E-cadherin. Also, we determined that PM-induced *Gt* increase within 3h is not a consequence of PM-induced cell death/injury in AEC. Furthermore, we show that the mitochondria is required for PM-induced occludin reduction at the plasma membrane, and overexpression of Manganese Superoxide Dismutase (MnSOD) and Catalase prevent the PM-induced *Gt* increase, as well as occludin reduction at the plasma membrane and occludin-ZO-1 dissociation in AEC.

PM with a diameter less than 10 μ m can penetrate the airways, but only smaller particles with an aerodynamic diameter of less than 2.5 μ m (PM_{2.5}) are capable to reach the alveolar space and potentially be responsible for injuring the alveolar epithelium. DEP has this size range and represents an important fraction of PM_{2.5}³³. Consistent with this, our results show

that DEP and PM₁₀ had similar effects on AEC, causing disruption of TJ and the alveolar barrier. Conversely, TiO₂, an inert particle, does not share any of the effects of PM₁₀ or DEP, suggesting that the composition of these particles, rather than the size, is responsible for the observed effects in AEC.

Occludin internalization occurs in response to cytokines, bacteria, toxins and calcium depletion^{34, 35}. Trafficking of occludin as well as its interaction with other proteins, such as ZO-1, is key in the regulation of TJ and paracellular permeability³⁶. Our results are consistent with other authors who have shown that occludin and its association with ZO-1, regulate epithelial barrier integrity³⁷⁻³⁹. Since localization of occludin at the plasma membrane is dependent on phosphorylation of different residues at its C terminal domain^{37, 40} we speculate that kinases activated by an increase in ROS production, such as PKC-zeta or MAPK^{41, 42}, can mediate the effects of PM on TJ, causing its dissociation from ZO-1 and the cytoskeleton, resulting in a loss of TJ integrity.

PM induces an inflammatory response in the lung as well as oxidative damage⁴³. Oxidative stress plays a central role in disruption of epithelial barriers, not only in the lung but in blood-brain and in the intestinal barrier^{44,45}. PM induces ROS generation in AEC, primarily from complex III of the mitochondrial electron transport chain²². It has been reported that redistribution of occludin and reorganization of TJ are induced by increased hydrogen peroxide (H₂O₂) in endothelial cells⁴². ROS plays a role mediating PM-induced effects, since cells are protected by overexpression of antioxidant enzymes and lack of mitochondrial ROS in p0 cells as observed in figures 5 and 7.

PM induces apoptosis of AEC and activation of cell death pathways is required for PM-induced increase in alveolar permeability^{25, 46}. Accordingly, our results support the hypothesis that PM-induced cell death seems to be associated to changes in permeability to larger molecules after 24 hours of PM exposure, while increases in paracellular permeability to ions occur earlier and are a consequence of TJ dysfunction and not cell death. These results suggest that PM impairs the alveolar epithelial barrier by different mechanisms. The implications of these results are related to previous reports that have shown that TJ dysfunction is associated with the development of inflammation³⁴. We consider that strategies to prevent PM-induced lung inflammation should take into consideration, not only the cell death machinery activated by air pollutants, but the effect of these particles on TJ integrity in the alveolar epithelial barrier.

In summary, our results support the hypothesis that PM triggers dissociation of occludin from ZO-1 and alveolar epithelial barrier dysfunction and these effects are prevented by overexpression of antioxidant enzymes.

Supplementary Material

Refer to Web version on PubMed Central for supplementary material.

Acknowledgments

Grant Information: This study was supported by K01HL080966 NHLBI and NIEHS/NIH P30 ES05605. We would like to thank Dr. Joseph Zabner for his suggestions.

References

1. Samet JM, Dominici F, Curriero FC, Coursac I, Zeger SL. Fine particulate air pollution and mortality in 20 U.S. cities, 1987-1994. *N Engl J Med.* 2000; 343:1742–9. [PubMed: 11114312]

2. Pope CA 3rd, Burnett RT, Thun MJ, Calle EE, Krewski D, et al. Lung cancer, cardiopulmonary mortality, and long-term exposure to fine particulate air pollution. *JAMA*. 2002; 287:1132–41. [PubMed: 11879110]
3. Pope CA 3rd, Burnett RT, Thurston GD, Thun MJ, Calle EE, et al. Cardiovascular mortality and long-term exposure to particulate air pollution: epidemiological evidence of general pathophysiological pathways of disease. *Circulation*. 2004; 109:71–7. [PubMed: 14676145]
4. Dominici F, McDermott A, Daniels M, Zeger SL, Samet JM. Revised analyses of the National Morbidity, Mortality, and Air Pollution Study: mortality among residents of 90 cities. *J Toxicol Environ Health A*. 2005; 68:1071–92. [PubMed: 16024489]
5. Katsouyanni K, Touloumi G, Samoli E, Gryparis A, Le Tertre A, et al. Confounding and effect modification in the short-term effects of ambient particles on total mortality: results from 29 European cities within the APHEA2 project. *Epidemiology*. 2001; 12:521–31. [PubMed: 11505171]
6. O'Connor GT, Neas L, Vaughn B, Kattan M, Mitchell H, et al. Acute respiratory health effects of air pollution on children with asthma in US inner cities. *J Allergy Clin Immunol*. 2008; 121:1133–9 e1. [PubMed: 18405952]
7. Sint T, Donohue JF, Ghio AJ. Ambient air pollution particles and the acute exacerbation of chronic obstructive pulmonary disease. *Inhal Toxicol*. 2008; 20:25–9. [PubMed: 18236218]
8. Regalado J, Perez-Padilla R, Sansores R, Paramo Ramirez JI, Brauer M, et al. The effect of biomass burning on respiratory symptoms and lung function in rural Mexican women. *Am J Respir Crit Care Med*. 2006; 174:901–5. [PubMed: 16799080]
9. Barry AC, Mannino DM, Hopenhayn C, Bush H. Exposure to Indoor Biomass Fuel Pollutants and Asthma Prevalence in Southeastern Kentucky: Results From the Burden of Lung Disease (BOLD) Study. *J Asthma*.
10. Izzotti A, Parodi S, Quaglia A, Fare C, Vercelli M. The relationship between urban airborne pollution and short-term mortality: quantitative and qualitative aspects. *Eur J Epidemiol*. 2000; 16:1027–34. [PubMed: 11421471]
11. Banauch GI, Hall C, Weiden M, Cohen HW, Aldrich TK, et al. Pulmonary function after exposure to the World Trade Center collapse in the New York City Fire Department. *Am J Respir Crit Care Med*. 2006; 174:312–9. [PubMed: 16645172]
12. Aldrich TK, Gustave J, Hall CB, Cohen HW, Webber MP, et al. Lung function in rescue workers at the World Trade Center after 7 years. *N Engl J Med*. 362:1263–72. [PubMed: 20375403]
13. Castranova V, Rabovsky J, Tucker JH, Miles PR. The alveolar type II epithelial cell: a multifunctional pneumocyte. *Toxicol Appl Pharmacol*. 1988; 93:472–83. [PubMed: 3285521]
14. Bush KT, Keller SH, Nigam SK. Genesis and reversal of the ischemic phenotype in epithelial cells. *J Clin Invest*. 2000; 106:621–6. [PubMed: 10974012]
15. Lehmann AD, Blank F, Baum O, Gehr P, Rothen-Rutishauser BM. Diesel exhaust particles modulate the tight junction protein occludin in lung cells in vitro. *Part Fibre Toxicol*. 2009; 6:26. [PubMed: 19814802]
16. Dobbs LG, Gonzalez R, Williams MC. An improved method for isolating type II cells in high yield and purity. *Am Rev Respir Dis*. 1986; 134:141–5. [PubMed: 3637065]
17. King MP, Attardi G. Isolation of human cell lines lacking mitochondrial DNA. *Methods Enzymol*. 1996; 264:304–13. [PubMed: 8965704]
18. Zabner J, Winter M, Excoffon KJ, Stoltz D, Ries D, et al. Histamine alters E-cadherin cell adhesion to increase human airway epithelial permeability. *J Appl Physiol*. 2003; 95:394–401. [PubMed: 12794099]
19. Lam EW, Zwacka R, Seftor EA, Nieva DR, Davidson BL, et al. Effects of antioxidant enzyme overexpression on the invasive phenotype of hamster cheek pouch carcinoma cells. *Free Radic Biol Med*. 1999; 27:572–9. [PubMed: 10490277]
20. Zwacka RM, Zhou W, Zhang Y, Darby CJ, Dudus L, et al. Redox gene therapy for ischemia/reperfusion injury of the liver reduces AP1 and NF-kappaB activation. *Nat Med*. 1998; 4:698–704. [PubMed: 9623979]
21. Mutlu GM, Snyder C, Bellmeyer A, Wang H, Hawkins K, et al. Airborne particulate matter inhibits alveolar fluid reabsorption in mice via oxidant generation. *Am J Respir Cell Mol Biol*. 2006; 34:670–6. [PubMed: 16439801]

22. Soberanes S, Urich D, Baker CM, Burgess Z, Chiarella SE, et al. Mitochondrial complex III-generated oxidants activate ASK1 and JNK to induce alveolar epithelial cell death following exposure to particulate matter air pollution. *J Biol Chem.* 2009; 284:2176–86. [PubMed: 19033436]
23. Upadhyay D, Panduri V, Ghio A, Kamp DW. Particulate matter induces alveolar epithelial cell DNA damage and apoptosis: role of free radicals and the mitochondria. *Am J Respir Cell Mol Biol.* 2003; 29:180–7. [PubMed: 12600817]
24. Holder AL, Lucas D, Goth-Goldstein R, Koshland CP. Cellular response to diesel exhaust particles strongly depends on the exposure method. *Toxicol Sci.* 2008; 103:108–15. [PubMed: 18227103]
25. Soberanes S, Panduri V, Mutlu GM, Ghio A, Bundinger GR, et al. p53 mediates particulate matter-induced alveolar epithelial cell mitochondria-regulated apoptosis. *Am J Respir Crit Care Med.* 2006; 174:1229–38. [PubMed: 16946128]
26. Breckenridge DG, Xue D. Regulation of mitochondrial membrane permeabilization by BCL-2 family proteins and caspases. *Curr Opin Cell Biol.* 2004; 16:647–52. [PubMed: 15530776]
27. Flynn AN, Itani OA, Moninger TO, Welsh MJ. Acute regulation of tight junction ion selectivity in human airway epithelia. *Proc Natl Acad Sci U S A.* 2009; 106:3591–6. [PubMed: 19208806]
28. Tunggal JA, Helfrich I, Schmitz A, Schwarz H, Gunzel D, et al. E-cadherin is essential for in vivo epidermal barrier function by regulating tight junctions. *EMBO J.* 2005; 24:1146–56. [PubMed: 15775979]
29. Emerling BM, Weinberg F, Snyder C, Burgess Z, Mutlu GM, et al. Hypoxic activation of AMPK is dependent on mitochondrial ROS but independent of an increase in AMP/ATP ratio. *Free Radic Biol Med.* 2009; 46:1386–91. [PubMed: 19268526]
30. Lecuona E, Minin A, Trejo HE, Chen J, Comellas AP, et al. Myosin-Va restrains the trafficking of Na⁺/K⁺-ATPase-containing vesicles in alveolar epithelial cells. *J Cell Sci.* 2009; 122:3915–22. [PubMed: 19808891]
31. Dagher Z, Garcon G, Billet S, Verdin A, Ledoux F, et al. Role of nuclear factor-kappa B activation in the adverse effects induced by air pollution particulate matter (PM2.5) in human epithelial lung cells (L132) in culture. *J Appl Toxicol.* 2007; 27:284–90. [PubMed: 17265450]
32. Comellas AP, Dada LA, Lecuona E, Pesce LM, Chandel NS, et al. Hypoxia-mediated degradation of Na,K-ATPase via mitochondrial reactive oxygen species and the ubiquitin-conjugating system. *Circ Res.* 2006; 98:1314–22. [PubMed: 16614303]
33. Schuetzle D. Sampling of vehicle emissions for chemical analysis and biological testing. *Environ Health Perspect.* 1983; 47:65–80. [PubMed: 6186484]
34. Simonovic I, Rosenberg J, Koutsouris A, Hecht G. Enteropathogenic *Escherichia coli* dephosphorylates and dissociates occludin from intestinal epithelial tight junctions. *Cell Microbiol.* 2000; 2:305–15. [PubMed: 11207587]
35. Yu D, Turner JR. Stimulus-induced reorganization of tight junction structure: the role of membrane traffic. *Biochim Biophys Acta.* 2008; 1778:709–16. [PubMed: 17915190]
36. Olivera D, Knall C, Boggs S, Seagrave J. Cytoskeletal modulation and tyrosine phosphorylation of tight junction proteins are associated with mainstream cigarette smoke-induced permeability of airway epithelium. *Exp Toxicol Pathol.* 2009
37. Suzuki T, Elias BC, Seth A, Shen L, Turner JR, et al. PKC ϵ regulates occludin phosphorylation and epithelial tight junction integrity. *Proc Natl Acad Sci U S A.* 2009; 106:61–6. [PubMed: 19114660]
38. Furuse M, Itoh M, Hirase T, Nagafuchi A, Yonemura S, et al. Direct association of occludin with ZO-1 and its possible involvement in the localization of occludin at tight junctions. *J Cell Biol.* 1994; 127:1617–26. [PubMed: 7798316]
39. Phillips BE, Cancel L, Tarbell JM, Antonetti DA. Occludin independently regulates permeability under hydrostatic pressure and cell division in retinal pigment epithelial cells. *Invest Ophthalmol Vis Sci.* 2008; 49:2568–76. [PubMed: 18263810]
40. Elias BC, Suzuki T, Seth A, Giorgianni F, Kale G, et al. Phosphorylation of Tyr-398 and Tyr-402 in occludin prevents its interaction with ZO-1 and destabilizes its assembly at the tight junctions. *J Biol Chem.* 2009; 284:1559–69. [PubMed: 19017651]

41. Li PF, Maasch C, Haller H, Dietz R, von Harsdorf R. Requirement for protein kinase C in reactive oxygen species-induced apoptosis of vascular smooth muscle cells. *Circulation*. 1999; 100:967–73. [PubMed: 10468528]
42. Kevil CG, Oshima T, Alexander B, Coe LL, Alexander JS. H₂O₂-mediated permeability: role of MAPK and occludin. *Am J Physiol Cell Physiol*. 2000; 279:C21–30. [PubMed: 10898713]
43. Li N, Sioutas C, Cho A, Schmitz D, Misra C, et al. Ultrafine particulate pollutants induce oxidative stress and mitochondrial damage. *Environ Health Perspect*. 2003; 111:455–60. [PubMed: 12676598]
44. Pun PB, Lu J, Moochhala S. Involvement of ROS in BBB dysfunction. *Free Radic Res*. 2009; 43:348–64. [PubMed: 19241241]
45. Schreibelt G, Kooij G, Reijkerk A, van Doorn R, Gringhuis SI, et al. Reactive oxygen species alter brain endothelial tight junction dynamics via RhoA, PI3 kinase, and PKB signaling. *FASEB J*. 2007; 21:3666–76. [PubMed: 17586731]
46. Urich D, Soberanes S, Burgess Z, Chiarella SE, Ghio AJ, et al. Proapoptotic Noxa is required for particulate matter-induced cell death and lung inflammation. *FASEB J*. 2009; 23:2055–64. [PubMed: 19237507]

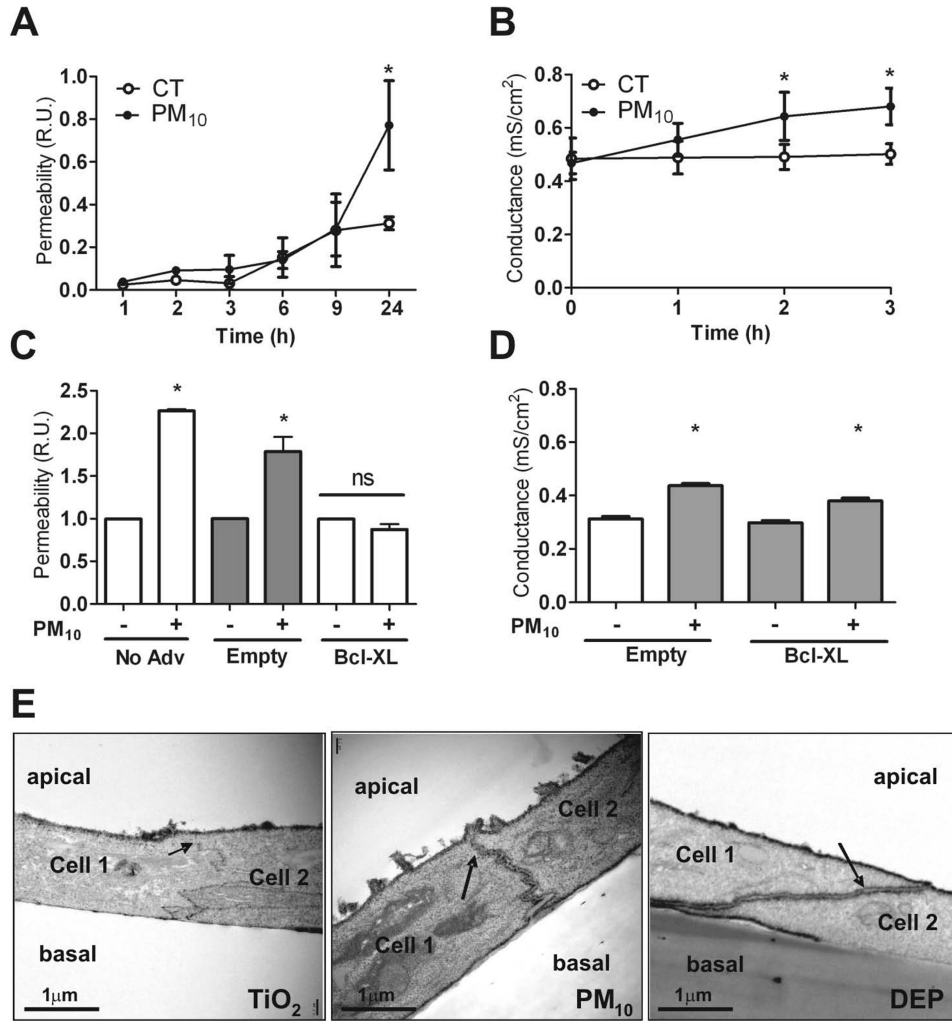


Figure 1. PM disrupts alveolar epithelial barrier

Panel A & B. Primary rat AEC were plated on inserts and at day 3 of isolation were treated with PM₁₀ (20 μg/cm²). Permeability to 4 kDa FITC-dextran (A) and *Gt* (B) were measured at different time points (1, 2, 3, 6, 9 & 24 hours). **Panel C & D.** 24 hours after infection of AEC with adenovirus containing Bcl-xL plasmid, cells were treated with PM₁₀ (20 μg/cm²) and permeability to FITC-dextran was measured at 24h (C) and *Gt* was determined at 3h after treatment with PM₁₀ (20 μg/cm²) (D). **Panel E.** Primary rat AEC were treated for 3h with 50 μg/cm² of TiO₂, PM₁₀ or DEP, they were then fixed and stained with La³⁺ on the apical side of the insert and observed under transmission electron microscopy. Electron dense La³⁺ penetrates the TJ (arrows) into the intercellular space after treatment with PM₁₀ and DEP but not with TiO₂. Graph represents mean ± SEM (n=3). * p<0.05 when compared with control.

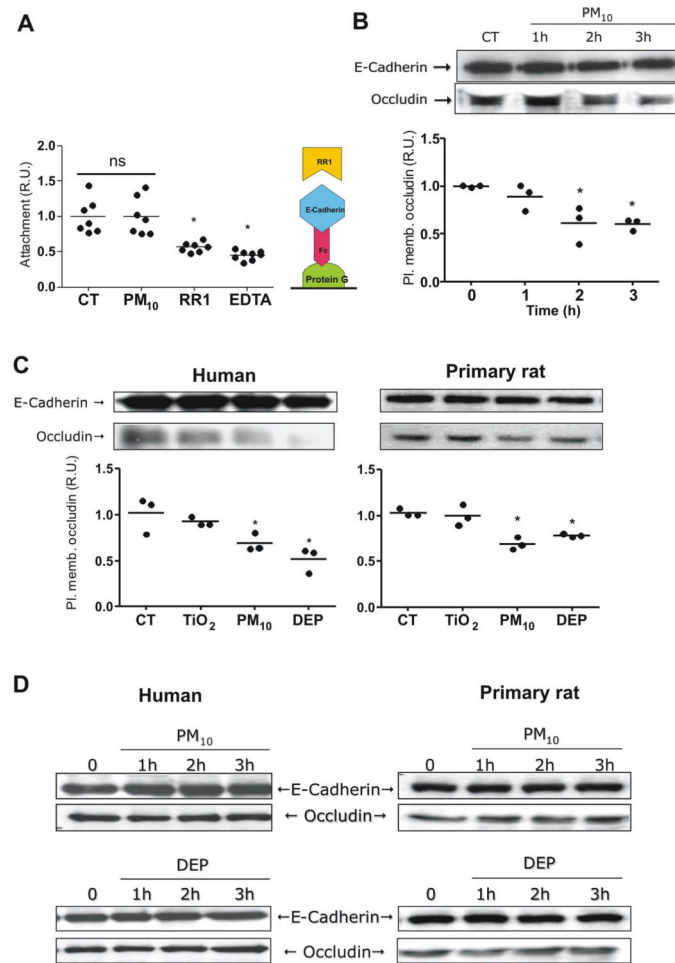


Figure 2. PM reduces occludin abundance at the plasma membrane in AEC

Panel A. Human AEC were treated with calcein-AM and allowed to attach to a protein G plate coated with E-cadherin-Fc chimera (schematic representation on the right). Cells were treated with PM₁₀ (20 μg/cm²) for 3h; wells then were washed and fluorescence of remaining cells was measured. **Panel B.** Human AEC were treated with PM₁₀ (20 μg/cm²) for 1, 2 and 3 hours, surface proteins were then labeled with biotin and pulled down with streptavidin beads, WB of these proteins is shown. **Panel C.** Human and primary rat AEC were treated with 20 μg/cm² of TiO₂, PM₁₀ or DEP and surface protein were labeled with biotin and pulled down with streptavidin beads and analyzed by WB. **Panel D.** Total cell lysate of human and rat AEC were analyzed by WB after treatment with PM₁₀ and DEP (50 μg/cm²). *Representative blots and quantitative analysis of three independent experiments are shown. Graph represents mean with dots representing each individual experiment. * p < 0.05 when compared with control.*

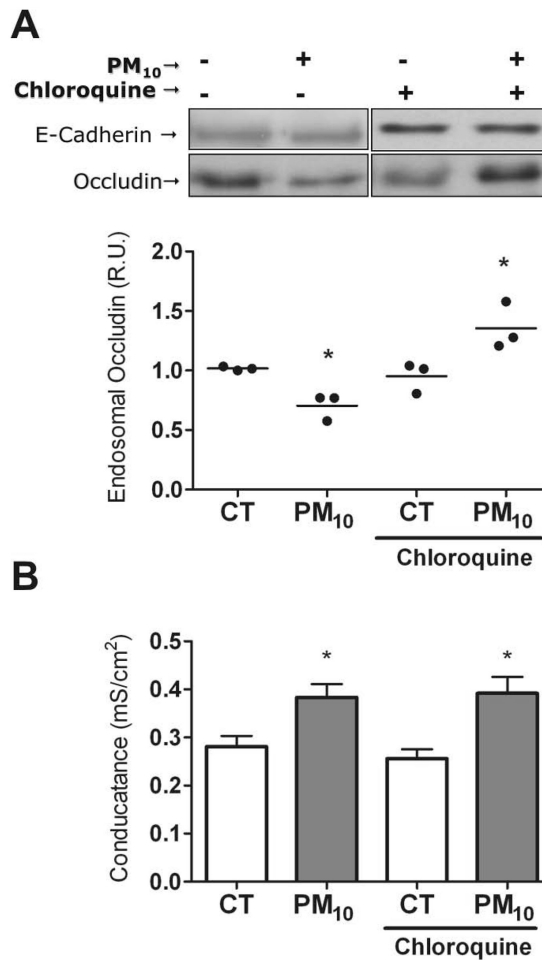


Figure 3. PM increases occludin abundance into the endosomal compartments in AEC
Panel A. AEC were treated with PM₁₀ (20 μ g/cm²) for 3h in the presence or absence of lysosome inhibitor chloroquine (100 μ M). Endosomal fraction was separated by sucrose gradient and occludin abundance was analyzed by WB. **Panel B.** Incubation with chloroquine (100 μ M) does not affect the PM-induced increase in AEC *Gt*. Shown are representative blots and quantitative analysis of three independent experiments. *Graph A* represents mean with dots representing each individual experiment and *Graph B* represents mean \pm SEM ($n=3$). * $p<0.05$ when compared with control.

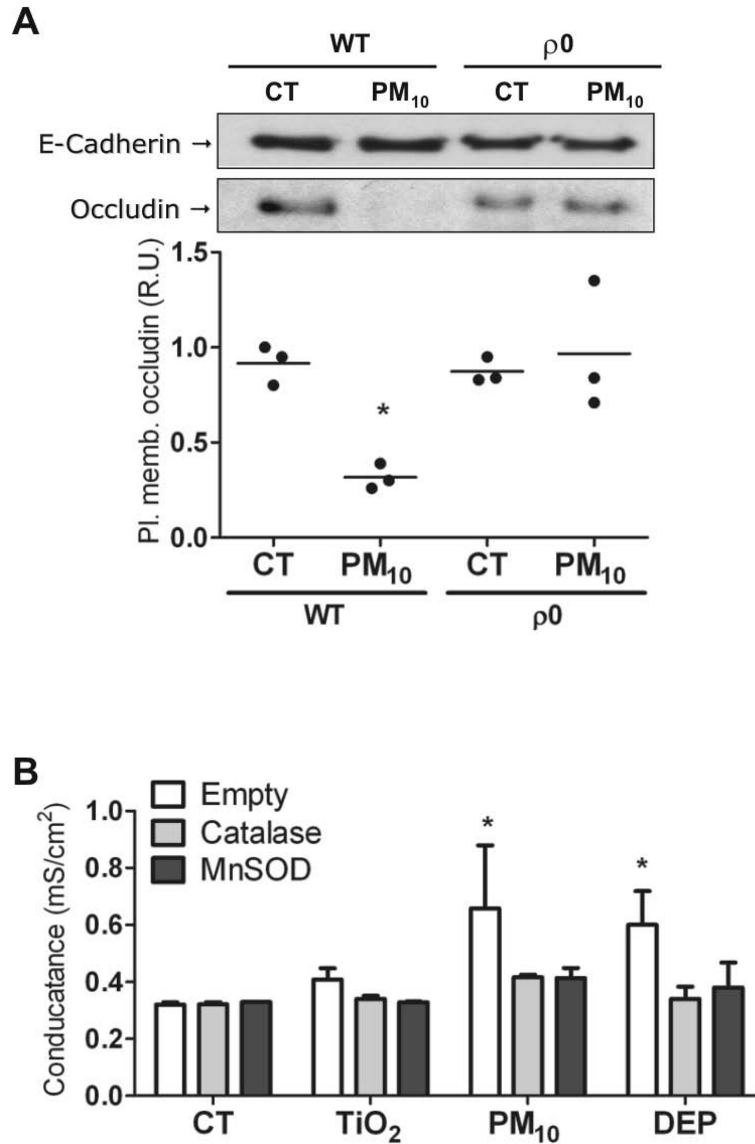


Figure 4. Mitochondrial ROS mediate PM-induced *Gt* increase and occludin reduction in AEC
Panel A. WT and ρ0 human AEC were treated with PM₁₀ (20μg/cm²) for 3h, then, surface proteins were labeled with biotin and pulled down with streptavidin beads and analyzed by WB. **Panel B.** Primary rat AEC were infected with adenovirus containing Catalase and MnSOD plasmids, 24h after infection, cells were treated with 20μg/cm² of TiO₂, PM₁₀ or DEP for 3h and *Gt* were measured. Shown are representative blots and quantitative analysis of three independent experiments. *Graph A* represents mean with dots representing individual experiments and *Graph B* represents mean ± SEM (n=3). *p<0.05 when compared with control.

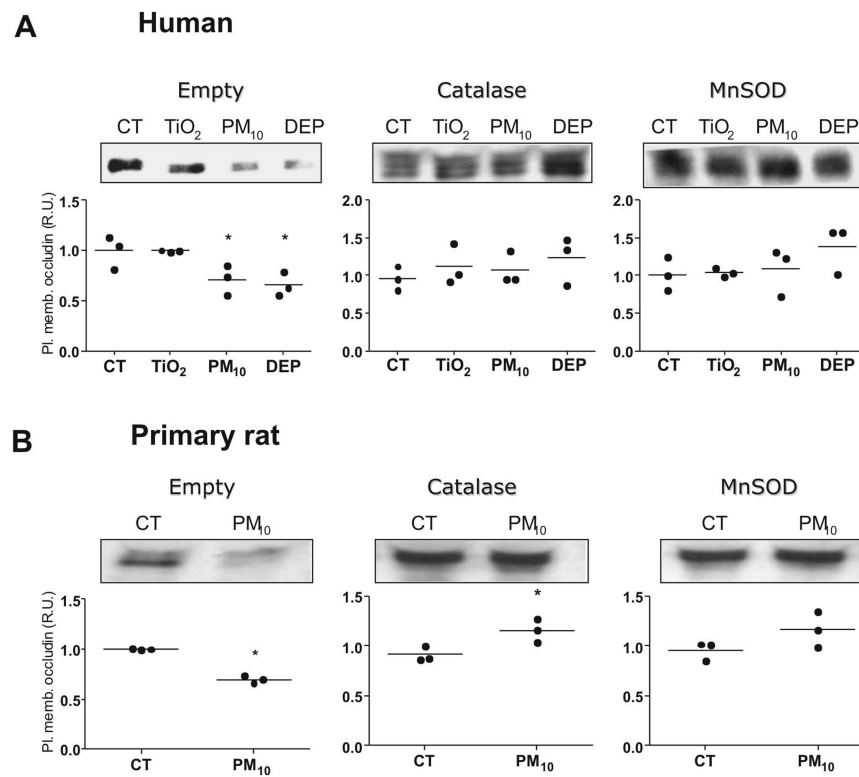


Figure 5. Overexpression of MnSOD and Catalase prevent PM-induced occludin reduction at the plasma membrane in AEC

Panel A & B. AEC were infected with empty adenovirus or adenovirus containing MnSOD and Catalase plasmids. 24h later, cells were exposed to PM ($50\mu\text{g}/\text{cm}^2$) for 3 h.

Overexpression of antioxidant enzymes prevent reduction of occludin at the plasma membrane after treatment with PM₁₀ and DEP in human (A) and primary rat (B) AEC.

Shown are representative blots and quantitative analysis of three independent experiments.

*Graph represents mean with dots representing individual experiments. * $p < 0.05$ when compared with control.*

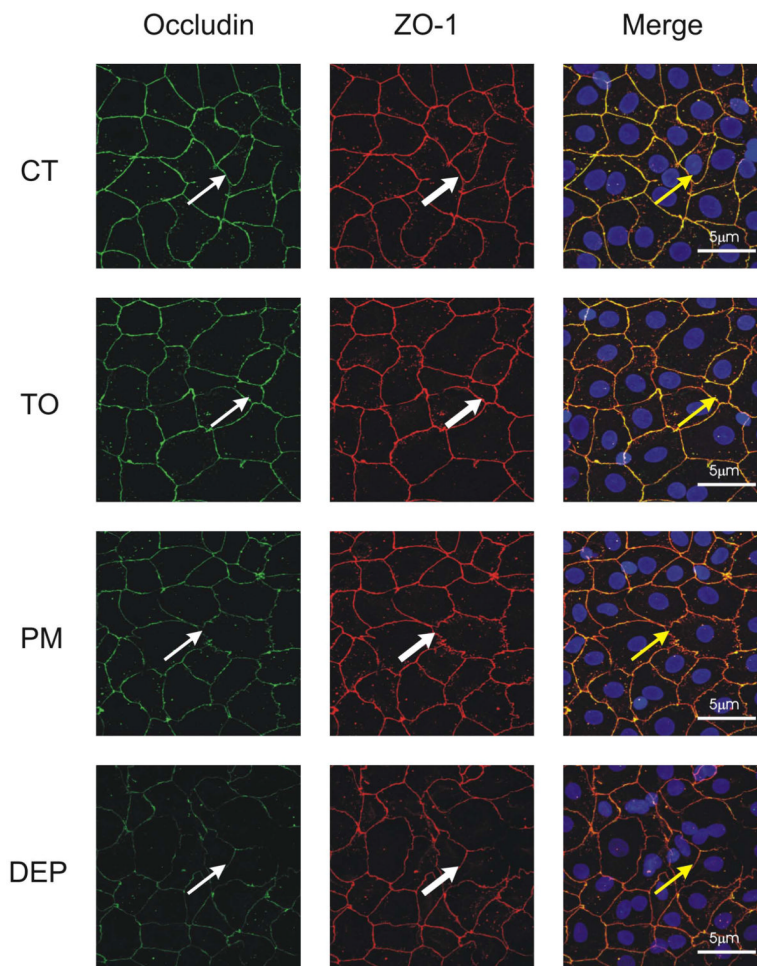


Figure 6. PM decreases colocalization of Occludin and ZO-1

Primary rat AEC treated with TiO_2 , PM_{10} or DEP ($50\mu\text{g}/\text{cm}^2$) for 3h were then fixed with anhydrous methanol and incubated with antibody against occludin (thin arrow) and ZO-1 (thick arrows), images were merged to assess colocalization (yellow arrows). *Images are representative of three independent experiments.*

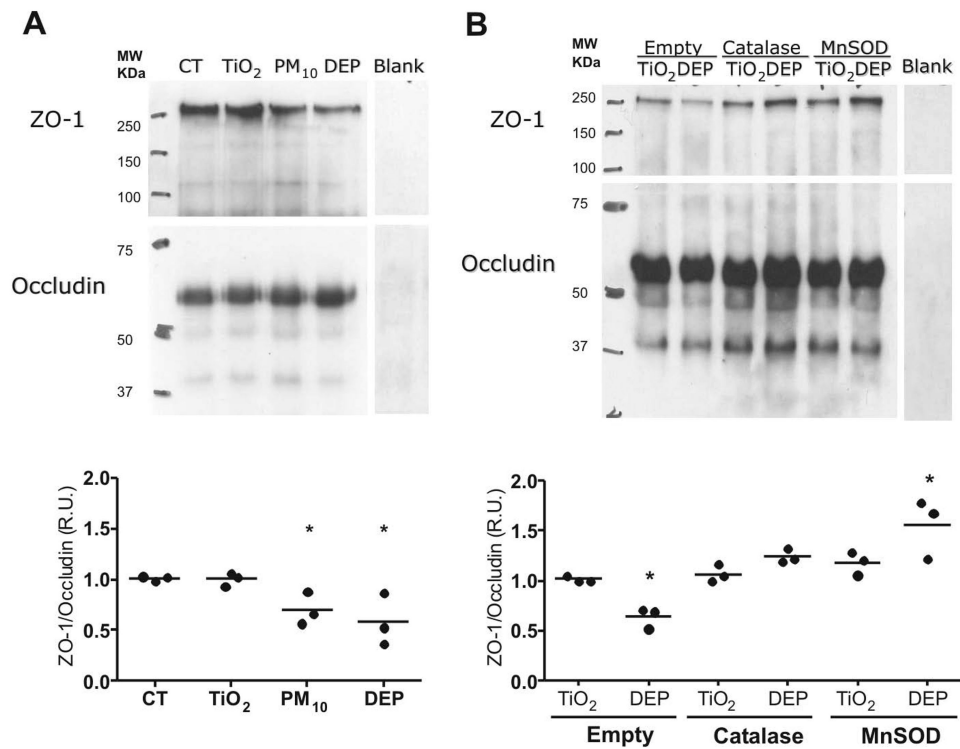


Figure 7. PM causes dissociation of Occludin and ZO-1

Panel A. Co-immunoprecipitation of occludin after treatment with of TiO₂, PM₁₀ or DEP (50μg/cm²) for 3h. Total cell lysate was incubated with polyclonal anti-occludin antibody and pull down with protein G agarose beads. Pulled down proteins were analyzed by WB.

Panel B. AEC were infected with empty adenovirus or adenovirus containing MnSOD and Catalase plasmids. 24h later, cells lysate were exposed to TiO₂ or DEP (50μg/cm²) for 3h. Co-immunoprecipitation of occludin was then performed. Total cell lysate was incubated with polyclonal anti-occludin antibody and pull down with protein G agarose beads. Pulled down proteins were analyzed by WB. *Shown are representative blots and quantitative analysis of three independent experiments. Graph represents mean with dots representing individual experiments. * p<0.05 when compared with TiO₂*